

# Sum rule approach to a soft dipole mode in $\Lambda$ hypernuclei

F. Minato<sup>1,2</sup> and K. Hagino<sup>3</sup>

<sup>1</sup> Nuclear Data Center, Japan Atomic Energy Agency, Tokai 319-1195, Japan

<sup>2</sup> Institut d'Astronomie et d'Astrophysique, Université Libre de Bruxelles,  
Campus de la Plaine CP 226, 1050, Brussels, Belgium

<sup>3</sup> Department of Physics, Tohoku University, Sendai 980-8578, Japan

(Dated: October 1, 2018)

Applying the sum rule approach, we investigate the energy of a soft dipole motion in  $\Lambda$  hypernuclei, which results from a dipole oscillation of a  $\Lambda$  hyperon against the core nucleus. To this end, we systematically study single- $\Lambda$  hypernuclei, from  ${}^{16}_{\Lambda}\text{O}$  to  ${}^{208}_{\Lambda}\text{Pb}$ , for which the ground state wave function is obtained in the framework of Hartree-Fock method with several Skyrme-type  $\Lambda N$  interactions. Our results indicate that the excitation energy of the soft dipole  $\Lambda$  mode,  $E_{sd\Lambda}$ , decreases as the mass number increases. We find that the excitation energy is well parametrized as  $E_{sd\Lambda} = 26.6A^{-1/3} + 11.2A^{-2/3}$  MeV as a function of mass number  $A$ .

PACS numbers: 21.80.+a, 21.60.Jz, 21.60.Ev, 23.20.-g

Hypernuclear physics has attracted lots of attention in recent years [1]. A  $\Lambda$  hyperon is free from the Pauli principle from nucleons, and thus can exist in a deep inside of a nucleus. Because of this property, a  $\Lambda$  hyperon provides various kinds of impurity effect on the core nucleus. One of the well-known examples is a shrinkage of intercluster distance in  ${}^7_{\Lambda}\text{Li}$  and  ${}^9_{\Lambda}\text{Be}$  [2–6]. Other examples include a disappearance of nuclear deformation due to a  $\Lambda$  hyperon [7–10], an influence on the triaxial degree of freedom [11, 12], and an increase of fission barrier height [13]. In addition to the static properties, a  $\Lambda$  hyperon can also alter nuclear dynamical motions. In particular, low-lying modes of excitation in  $\Lambda$  hypernuclei have been studied with cluster model [14], ab-initio few-body calculations [15, 16], shell model [17], 5-dimensional (5D) collective Bohr Hamiltonian [18], and anti-symmetrized molecular dynamics (AMD)[12]. Together with experimental data, those theoretical studies would help us to understand not only the impurity effect on nuclear structure but also the characteristics of an effective  $\Lambda N$  interaction.

In our previous study, we studied multipole vibrational motions of  $\Lambda$  hypernuclei using random-phase approximation (RPA) [19]. We have predicted a novel dipole mode, which we call the soft dipole  $\Lambda$  mode, in a double- $\Lambda$  hypernucleus  ${}^{18}_{\Lambda\Lambda}\text{O}$  [19]. This mode appears in the low energy region, and its strength is almost concentrated in a single peak with a magnitude of about a quarter of that of the giant dipole resonance (with the peak height in the strength distribution being about a half of that for the giant dipole resonance). A similar peak appears neither in other multipolarities nor in the dipole motion of the normal nucleus,  ${}^{16}\text{O}$ . From the transition density, we argued that this mode corresponds to a dipole oscillation of the two  $\Lambda$  hyperons against the core nucleus. Notice that this is similar to the soft dipole motion in neutron-rich halo nuclei [20], in which weakly bound valence neutrons oscillate against the core nucleus.

In this paper, we systematically study the soft dipole  $\Lambda$  mode from light to heavy hypernuclei. In order to estimate the excitation energy of the soft dipole  $\Lambda$  mode,

we employ the sum rule approach [21–23]. This approach provides a convenient way to estimate the excitation energy, as it can be evaluated only with the ground state wave function. This enables one to study the soft dipole  $\Lambda$  mode in single- $\Lambda$  hypernuclei, whereas an application of RPA to single- $\Lambda$  hypernuclei is much more complicated due to the broken time-reversal symmetry and half-integer spins.

In the sum rule approach, the moments of the strength distribution are expressed in terms of the ground state expectation value of certain operators [24, 25]. In order to apply this approach, we thus first obtain the wave function for the ground state of hypernuclei by adopting the Hartree-Fock method with a Skyrme-type zero-range force as an effective  $\Lambda N$  interaction. The  $\Lambda N$  and 3-body  $\Lambda NN$  interactions then read [26],

$$\begin{aligned} v_{\Lambda N}(\mathbf{r}_{\Lambda} - \mathbf{r}_N) &= t_0^{\Lambda}(1 + x_0^{\Lambda}P_{\sigma})\delta(\mathbf{r}_{\Lambda} - \mathbf{r}_N) \\ &+ \frac{1}{2}t_1^{\Lambda}\left(\mathbf{k}'^2\delta(\mathbf{r}_{\Lambda} - \mathbf{r}_N) + \delta(\mathbf{r}_{\Lambda} - \mathbf{r}_N)\mathbf{k}^2\right) \\ &+ t_2^{\Lambda}\mathbf{k}'\delta(\mathbf{r}_{\Lambda} - \mathbf{r}_N) \cdot \mathbf{k} + iW_0^{\Lambda}\mathbf{k}'\delta(\mathbf{r}_{\Lambda} - \mathbf{r}_N) \cdot (\boldsymbol{\sigma} \times \mathbf{k}) \end{aligned} \quad (1)$$

and

$$v_{\Lambda NN}(\mathbf{r}_{\Lambda}, \mathbf{r}_{N_1}, \mathbf{r}_{N_2}) = t_3^{\Lambda}\delta(\mathbf{r}_{\Lambda} - \mathbf{r}_{N_1})\delta(\mathbf{r}_{\Lambda} - \mathbf{r}_{N_2}), \quad (2)$$

respectively. Here,  $P_{\sigma}$  is the spin exchange operator, and the operator  $\mathbf{k}' = -(\nabla_1 - \nabla_2)/2i$  acts on the left hand side while  $\mathbf{k} = (\nabla_1 - \nabla_2)/2i$  acts on the right hand side. See Refs. [19, 26, 27] for the details of the Hartree-Fock method for hypernuclei.

The operator for the electric dipole (E1) response for single- $\Lambda$  hypernuclei is given by

$$\hat{F}_{\mu} = e \sum_{i \in p} (r_i Y_{1\mu}(\hat{r}_i) - R Y_{1\mu}(\mathbf{R})), \quad (3)$$

where

$$\mathbf{R} = \frac{1}{M} \left( m \sum_{i \in n.p} \mathbf{r}_i + m_{\Lambda} \mathbf{r}_{\Lambda} \right) \quad (4)$$

is the center of mass of the hypernucleus. Here,  $M \equiv m(Z + N) + m_\Lambda$  is the total mass of the hypernuclei,  $m = (m_p + m_n)/2 = 938.92 \text{ MeV}/c^2$  and  $m_\Lambda = 1115.68 \text{ MeV}/c^2$  being the mass of nucleon and  $\Lambda$  hyperon, respectively.  $N$  and  $Z$  are the number of neutron and proton, respectively.

We rearrange the E1 operator, Eq. (3), as

$$\hat{F}_\mu = \hat{F}_\mu^{(\text{core})} + \hat{F}_\mu^{(\Lambda)}, \quad (5)$$

with

$$\hat{F}_\mu^{(\text{core})} = e \left( \frac{N}{N+Z} \sum_{i \in p} r_i Y_{1\mu}(\hat{r}_i) - \frac{Z}{N+Z} \sum_{i \in n} r_i Y_{1\mu}(\hat{r}_i) \right), \quad (6)$$

and

$$\hat{F}_\mu^{(\Lambda)} = -e \frac{Z m_\Lambda}{M} \left( r_\Lambda Y_{1\mu}(\hat{r}_\Lambda) - R_c Y_{1\mu}(\hat{R}_c) \right), \quad (7)$$

where

$$\mathbf{R}_c = \frac{1}{N+Z} \sum_{i \in n,p} \mathbf{r}_i \quad (8)$$

is the center of mass of the core nucleus. The operator  $\hat{F}_\mu^{(\Lambda)}$  given by Eq. (7) is the E1 operator which induces the dipole motion between the  $\Lambda$  particle and the core nucleus, while  $\hat{F}_\mu^{(\text{core})}$ , Eq. (6), is identical to the usual E1 operator, which generates an oscillation between protons and neutrons in a normal nucleus.

The soft dipole  $\Lambda$  mode is interpreted as the vibration for the relative motion between the  $\Lambda$  hyperon and the core nucleus, as we have confirmed with RPA [19]. We thus estimate its energy by using the sum rules for the operator  $\hat{F}_\mu^{(\Lambda)}$ . The energy weighted sum rule can then be calculated using the Hamiltonian  $\hat{H}$  and the wave function of the ground state,  $|0\rangle$ , as

$$\begin{aligned} m_1^\Lambda &= \frac{1}{2} \langle 0 | \left[ \hat{F}_0^{(\Lambda)}, \left[ H, \hat{F}_0^{(\Lambda)} \right] \right] | 0 \rangle, \quad (9) \\ &= \frac{3e^2}{4\pi} \left( \frac{Z m_\Lambda}{M} \right)^2 \left[ \frac{\hbar^2}{2m_\Lambda} + \frac{\hbar^2}{2m_N(N+Z)} \right. \\ &\quad \left. + \frac{1}{4} (t_1^\Lambda + t_2^\Lambda) \left( 1 + \frac{1}{N+Z} \right)^2 \int \rho_\Lambda(\mathbf{r}) \rho_c(\mathbf{r}) d\mathbf{r} \right], \quad (10) \end{aligned}$$

where  $\rho_c(\mathbf{r}) \equiv \rho_p(\mathbf{r}) + \rho_n(\mathbf{r})$  and  $\rho_\Lambda(\mathbf{r})$  are the density distributions for the core nucleus and for the  $\Lambda$  particle, respectively. On the other hand, the non-energy weighted

sum rule for the soft dipole  $\Lambda$  mode is simply given by

$$\begin{aligned} m_0^\Lambda &= \sum_\nu \left| \langle \nu | \hat{F}_0^{(\Lambda)} | 0 \rangle \right|^2 = \langle 0 | \left( \hat{F}_0^{(\Lambda)} \right)^2 | 0 \rangle \\ &\simeq \left( e \frac{Z m_\Lambda}{M} \right)^2 \left[ \int \rho_\Lambda(r_\Lambda) (r_\Lambda Y_{10}(\hat{r}_\Lambda))^2 dr_\Lambda \right. \\ &\quad \left. + \int \rho_c(\mathbf{r}) \frac{1}{(N+Z)^2} (r Y_{10}(\hat{r}))^2 d\mathbf{r} \right] \quad (11) \\ &= \frac{e^2}{4\pi} \left( \frac{Z m_\Lambda}{M} \right)^2 \left( \langle r^2 \rangle_\Lambda + \frac{1}{(N+Z)^2} \langle r^2 \rangle_c \right), \end{aligned}$$

where  $\sqrt{\langle r^2 \rangle_\Lambda}$  and  $\sqrt{\langle r^2 \rangle_c}$  are the root mean square (rms) radius of the  $\Lambda$  hyperon and the core nucleus, respectively. Here, we have assumed the perfect decoupling between the soft dipole  $\Lambda$  mode and the giant dipole resonance[21]. The excitation energy for the soft dipole  $\Lambda$  mode is then estimated as  $E_{sd\Lambda} = m_1^\Lambda/m_0^\Lambda$ .

Let us now numerically evaluate the energy of the soft dipole  $\Lambda$  mode and discuss its mass number dependence. To this end, we study the following nine hypernuclei:  ${}^{16}_\Lambda\text{O}$ ,  ${}^{32}_\Lambda\text{S}$ ,  ${}^{40}_\Lambda\text{Ca}$ ,  ${}^{51}_\Lambda\text{V}$ ,  ${}^{64}_\Lambda\text{Ni}$ ,  ${}^{89}_\Lambda\text{Y}$ ,  ${}^{120}_\Lambda\text{Sn}$ ,  ${}^{139}_\Lambda\text{La}$  and  ${}^{208}_\Lambda\text{Pb}$ . We employ the  $\Lambda N$  forces constructed in Ref. [28], while we use the SkM\* set [29] for the  $NN$  interaction. There are 6 parameter sets for the  $\Lambda N$  interaction, No. 1-6, in which the sets No. 1, 2, 5, and 6 include the 3-body term proportional to  $t_3^\Lambda$  while No. 3 and No. 4 do not. The 3-body term, which works repulsively in general, significantly affects the  $\Lambda$  binding energy. For instance, one finds in Tab. I of Ref. [28] that the No. 1, 2, 5, and 6 sets provide a relatively shallow potential depth in nuclear matter  $D_\Lambda$ , among which the No. 2 set binds a  $\Lambda$  hyperon most weakly ( $D_\Lambda = 26.5 \text{ MeV}$ ). On the other hand, the No. 3 and 4 sets without the 3-body term lead to a deeper potential depth ( $D_\Lambda = 32.6$  and  $34.6 \text{ MeV}$ , respectively).

In solving the Hartree-Fock equations, we assume spherical symmetry for all the nuclei considered in this paper. For odd-mass nuclei, we employ the filling-approximation [30, 31], with which the last occupied orbit is filled only partially so as to reproduce the particle number of the whole system. For the  $\Lambda$  hyperon, we assume that it occupies the  $1s_{1/2}$  state with the occupation probability of one half.

We first discuss the rms radius for the  $\Lambda$  hyperon,  $\sqrt{\langle r^2 \rangle_\Lambda}$ , to which the non-energy weighted sum rule,  $m_0^\Lambda$ , is strongly related. Figure 1 shows  $\sqrt{\langle r^2 \rangle_\Lambda}$  as a function of  $A$ , where the results with those  $\Lambda N$  interactions with the 3-body term (that is, the No. 1,2,5, and 6 sets) are denoted by open symbols while those without it (that is, No. 3 and 4 sets) are by filled symbols. Since the radius of the core nucleus increases with its mass number, it is natural that the rms radius for the  $\Lambda$  hyperon,  $\sqrt{\langle r^2 \rangle_\Lambda}$ , also increases as a function of the mass number,  $A$ . One can see that the calculated radii show a clear dependence on the  $\Lambda N$  interaction adopted. In particular, the interactions with the 3-body term (*i.e.*, No. 1,

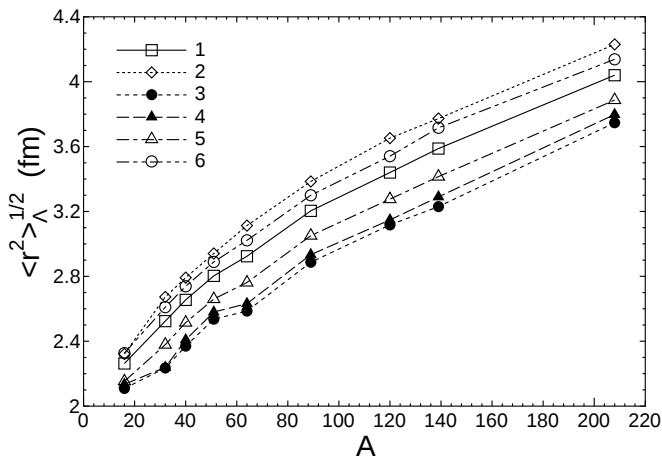


FIG. 1: The root mean square radius  $\sqrt{\langle r^2 \rangle_\Lambda}$  for the  $\Lambda$  hyperon in single- $\Lambda$  hypernuclei as a function of the mass number  $A$ , obtained with the Skyrme-Hartree-Fock calculations with six different  $\Lambda N$  interactions.

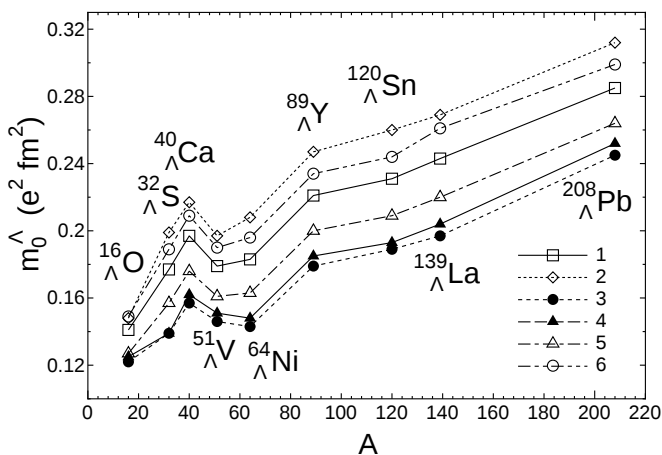


FIG. 2: The non-energy weighted sum rule for the soft dipole  $\Lambda$  mode as a function of mass number  $A$  calculated with six different  $\Lambda N$  interactions.

2, 5 and 6) yield a larger radius than those without it (*i.e.*, No. 3 and 4). This is because the  $\Lambda$  binding energy calculated with the No. 1, 2, 5 and 6 sets is smaller than that with the No. 3 and 4 sets. As a consequence, the density distribution of the  $\Lambda$  hyperon tends to expand outward. Notice that the No. 2 interaction having the largest  $t_3^\Lambda$  ( $= 3000 \text{ MeV}\cdot\text{fm}^6$ ) leads to the largest radii.

Figure 2 shows the non-energy weighted sum rule,  $m_0^\Lambda$ . On average, it increases with the mass number  $A$ , similarly to the rms radii shown in Fig. 1. It is also similar to the rms radii that the interactions with the 3-body term yield relatively larger values for  $m_0^\Lambda$ . However, in contrast to the rms radii, which increases monotonically as a function of  $A$ , the non-energy weighted sum rule  $m_0^\Lambda$  shows a non-monotonic behavior at  $^{51}\Lambda\text{V}$  and  $^{64}\Lambda\text{Ni}$ . This can be attributed to the fact that the factor  $(Zm_\Lambda/M)^2$  in Eq. (11) decreases from  $^{40}\Lambda\text{Ca}$  to  $^{51}\Lambda\text{V}$ , and then to  $^{64}\Lambda\text{Ni}$  due to the deviation from the  $N = Z$  line (to be more

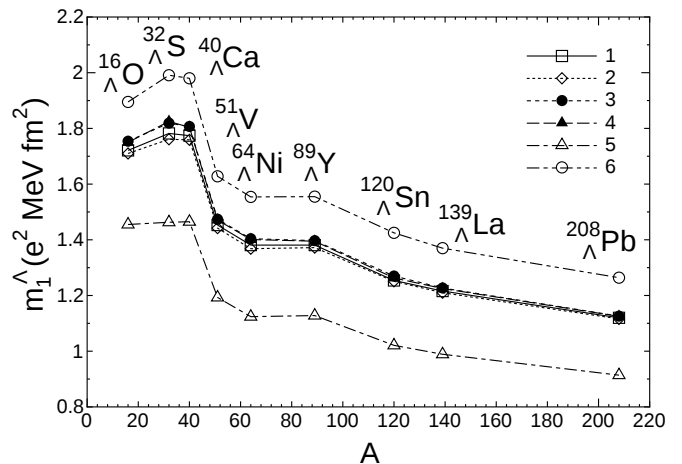


FIG. 3: The energy weighted sum rule for the soft dipole  $\Lambda$  mode in single- $\Lambda$  hypernuclei as a function of mass number  $A$ .

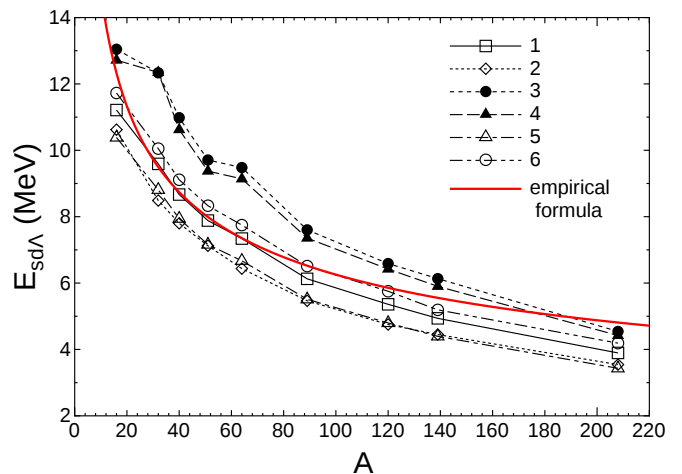


FIG. 4: (Color online) The excitation energy of the soft  $\Lambda$  dipole mode,  $E_{sd\Lambda}$ , obtained with the sum rule approach as  $E_{sd\Lambda} = m_1^\Lambda/m_0^\Lambda$ . The thick solid line indicates the results of the empirical formula given by Eq. (12).

precise, it is the  $N - 1 = Z$  line). That is, the value of  $(Zm_\Lambda/M)^2$  is 0.591, 0.534, and 0.518 for  $^{40}\Lambda\text{Ca}$ ,  $^{51}\Lambda\text{V}$ , and  $^{64}\Lambda\text{Ni}$ , respectively.

The energy weighted sum rule  $m_1^\Lambda$  is shown in Fig. 3. The No. 1-4 interactions show almost identical lines, as the coefficient of the third term in Eq. (10),  $a_1 = (t_1^\Lambda + t_2^\Lambda)/4$ , is identical for these sets (that is,  $a_1 = 26.3 \text{ MeV}\cdot\text{fm}^5$ ) [28]. On the other hand,  $a_1 = 0$  and  $45.0 \text{ MeV}\cdot\text{fm}^5$  for the No. 5 and 6 parameter sets, respectively, and these parameter sets yield the lowest and the largest value for  $m_1^\Lambda$ , respectively. A large decrease of  $m_1^\Lambda$  from  $^{40}\Lambda\text{Ca}$  to  $^{51}\Lambda\text{V}$  is again attributed to the decrease of the factor  $(Zm_\Lambda/M)^2$  in Eq. (10) due to the deviation from the  $N = Z$  line.

The energy of the soft dipole  $\Lambda$  mode,  $E_{sd\Lambda}$ , calculated with  $m_0^\Lambda$  and  $m_1^\Lambda$ , is shown in Fig. 4. Because of the minor contribution of the second term in Eq. (11) as

well as a cancellation of the factor  $(Z/M)^2$  between  $m_1^\Lambda$  and  $m_0^\Lambda$ , the energy  $E_{sd\Lambda}$  is almost inversely proportional to  $\langle r^2 \rangle_\Lambda$ . As a result, the No. 3 and 4 sets for the  $\Lambda N$  interaction, giving small root mean square radii, show large values for  $E_{sd\Lambda}$ , while the sets No. 1, 2, 5 and 6 provide small values of  $E_{sd\Lambda}$ . For all the  $\Lambda N$  interactions, the energy of the soft dipole  $\Lambda$  mode,  $E_{sd\Lambda}$ , decreases with the mass number  $A$  as expected. Assuming that the soft dipole  $\Lambda$  mode is close to a single particle excitation of the  $\Lambda$  hyperon in a harmonic oscillator potential, the mass number dependence of  $E_{sd\Lambda}$  may be parametrized as

$$E_{sd\Lambda} = \alpha A^{-1/3} + \beta A^{-2/3}. \quad (12)$$

By performing the least square fit to all the data points obtained with the six different  $\Lambda N$  interactions, we obtain the coefficients of the empirical formula as  $\alpha=26.6$  MeV and  $\beta = 11.2$  MeV. The energy obtained with this empirical formula is shown in Fig. 4 by the thick solid line. It well reproduces the average behavior of the excitation energy of the soft dipole  $\Lambda$  mode, even though it somewhat overestimates the energy for the  $^{208}_{\Lambda}\text{Pb}$  nucleus.

Shell model calculations with a meson-exchange YN interaction have been carried out for low-lying excited states in  $^{16}_{\Lambda}\text{O}$  [32] and  $^{40}_{\Lambda}\text{Ca}$  [33]. The soft dipole  $\Lambda$  mode appears in these calculations at around 10 MeV and 8-9 MeV for  $^{16}_{\Lambda}\text{O}$  and  $^{40}_{\Lambda}\text{Ca}$ , respectively, although the nature of the soft dipole  $\Lambda$  mode was not discussed in Refs. [32, 33]. These results are in a reasonable agreement with our results obtained with the parameter sets which include the three-body  $\Lambda NN$  interaction, that is, No. 1,2,5, and 6.

In summary, we have discussed the soft dipole  $\Lambda$  mode in single- $\Lambda$  hypernuclei using the sum rule approach. We have found that the non-energy weighted sum rule,  $m_0^\Lambda$ , for the soft dipole  $\Lambda$  mode depends significantly on the  $\Lambda N$  interaction. In particular, the  $\Lambda N$  interactions with the 3-body term leads to smaller values of  $m_0^\Lambda$  as compared to those without the 3-body term. On the other hand, the energy weighted sum rule,  $m_1^\Lambda$ , has a strong dependence on the momentum-dependent terms in the  $\Lambda N$  interaction. We have argued that the excitation energy of the soft dipole  $\Lambda$  mode is almost inversely proportional to the mean square radius and decreases with mass number. We have derived an empirical formula for the excitation energy, that scales as  $E_{sd\Lambda} = 26.2A^{-1/3} + 11.2A^{-2/3}$  MeV.

Our calculations indicate that the soft dipole  $\Lambda$  mode appears at around 10 MeV in  $^{16}_{\Lambda}\text{O}$ , which is in agreement with a shell model calculation with a meson exchange YN interaction. Although the core nucleus,  $^{15}\text{O}$ , is unstable and all the levels are not known exactly, the strength of the soft dipole  $\Lambda$  mode of  $^{16}_{\Lambda}\text{O}$  is strong, and it could be distinguished experimentally from the other levels associated with the core excitation. In heavier hypernuclei, the energy of the soft dipole mode decreases, and for *e.g.*,  $^{208}_{\Lambda}\text{Pb}$  it appears at around 4 MeV. In this energy region, there are only 40 discrete levels observed in the core nucleus,  $^{207}\text{Pb}$  [34]. One can thus have a hope to experimentally identify the soft dipole  $\Lambda$  mode in single- $\Lambda$  hypernuclei. It would be extremely interesting if such measurement could be realized in some future.

This work was supported by JSPS KAKENHI Grant Numbers 22540262 and 25105503.

- 
- [1] O. Hashimoto and H. Tamura, Prog. Part. Nucl. Phys. **57**, 564 (2006), and the references therein.
- [2] K. Tanida *et al.*, Phys. Rev. Lett. **86**, 1982 (2001).
- [3] H. Akikawa *et al.*, Phys. Rev. Lett. **88**, 082501 (2002); H. Tamura *et al.*, Nucl. Phys. **A754**, 58 (2005).
- [4] T. Motoba, H. Bando, and K. Ikeda, Prog. Theor. Phys. **70**, 189 (1983).
- [5] E. Hiyama, M. Kamimura, K. Miyazaki, and T. Motoba, Phys. Rev. **C59**, 2351 (1999).
- [6] K. Hagino and T. Koike, Phys. Rev. **C84**, 064325 (2011).
- [7] Myaing Thi Win and K. Hagino, Phys. Rev. **C78**, 054311 (2008).
- [8] H.-J. Schulze, Myaing Thi Win, K. Hagino, and H. Sagawa, Prog. Theo. Phys. **123**, 569 (2010).
- [9] B.-N. Lu, E.-G. Zhao, and S.-G. Zhou, Phys. Rev. **C84**, 014328 (2011).
- [10] M. Isaka, M. Kimura, A. Dote, and A. Ohnishi, Phys. Rev. **C83**, 044323 (2011).
- [11] Myaing Thi Win, K. Hagino, and T. Koike, Phys. Rev. **C83**, 014301 (2011).
- [12] M. Isaka, M. Kimura, A. Dote, and A. Ohnishi, Phys. Rev. **C83**, 054304 (2011); M. Isaka, H. Homma, M. Kimura, A. Dote, and A. Ohnishi, Phys. Rev. **C85**, 034303 (2012).
- [13] F. Minato, S. Chiba, and K. Hagino, Nucl. Phys. **A831**, 150 (2009); F. Minato and S. Chiba, Nucl. Phys. **A856**, 55 (2011).
- [14] E. Hiyama, M. Kamimura, T. Motoba, T. Yamada, and Y. Yamamoto, Phys. Rev. **C 66**, 024007 (2002); E. Hiyama, M. Kamimura, Y. Yamamoto, and T. Motoba, Phys. Rev. Lett. **104**, 212502 (2010).
- [15] H. Nemura, Y. Akaishi, and Y. Suzuki, Phys. Rev. Lett. **89**, 142504 (2002).
- [16] H. Nemura, S. Shinmura, Y. Akaishi, and Khin Swe Myint, Phys. Rev. Lett., **94**, 202502 (2005).
- [17] A. Gal, D.J. Millener, Phys. Lett. **B701**, 342 (2011).
- [18] J.M. Yao, Z.P. Li, K. Hagino, M. Thi Win, Y. Zhang, and J. Meng, Nucl. Phys. **A868-869**, 12 (2011).
- [19] F. Minato and K. Hagino, Phys. Rev. **C85**, 024316 (2012).
- [20] K. Ikeda, T. Myo, K. Kato, and H. Toki, Lecture Notes in Physics **818**, 165 (2010).
- [21] H. Sagawa and M. Honma, Phys. Lett. **B251**, 17 (1990).
- [22] H. Sagawa, N. Takigawa, and Nguyen Van Giai, Nucl.

- Phys. **A543**, 575 (1992).
- [23] H. Kurasawa and T. Suzuki, Prog. Theo. Phys. **94**, 931 (1995).
- [24] P. Ring and P. Schuck, *The Nuclear Many-Body Problem* (Springer-Verlag, Berlin, 1980).
- [25] O. Bohigas, A.M. Lane, and J. Martorell, Phys. Rep. **51**, 267 (1979).
- [26] M. Rayet, Ann. of Phys. **102**, 226 (1976); M. Rayet, Nucl. Phys. **A367**, 381 (1981).
- [27] D.E. Lanskoy, Phys. Rev. **C58**, 3351 (1998).
- [28] Y. Yamamoto, H. Bando, and J. Zofka, Prog. Theor. Phys. **80**, 757 (1988).
- [29] J. Bartel, P. Quentin, M. Brack, C. Guet, and H.B. Hakansson, Nucl. Phys. **A386**, 79 (1982).
- [30] S. Perez-Martin and L.M. Robledo, Phys. Rev. **C78**, 014304 (2008).
- [31] G.F. Bertsch, C.A. Bertulani, W. Nazarewicz, N. Schunck, and M.V. Stoitsov, Phys. Rev. **C79**, 034306 (2009).
- [32] Yiharn Tzeng, S.Y. Tsay Tzeng, T.T.S. Kuo, T.-S.H. Lee, and V.G.D. Stoks, Phys. Rev. **C61**, 031305 (R) (2000);
- [33] Yiharn Tzeng, S.Y. Tsay Tzeng, T.T.S. Kuo, Phys. Rev. **C65**, 047303 (2002).
- [34] National Nuclear Data Center, "NUDAT 2.5 Database," <http://www.nndc.bnl.gov/nudat2>.